Apical and Basolateral Endosomes of MDCK Cells Are Interconnected and Contain a Polarized Sorting Mechanism

Greg Odorizzi,* Adele Pearse,‡ Derrick Domingo,* Ian S. Trowbridge,* and Colin R. Hopkins‡

*Department of Cancer Biology, The Salk Institute for Biological Studies, San Diego, California 92186-5800; and ‡Medical Research Council Laboratory for Molecular Cell Biology, University College London, London WC1E 6BT England

Abstract. We have evaluated transcytotic routes in MDCK cells for their ability to generate a polarized surface distribution of trafficking proteins by following the intracellular sorting of transferrin receptors (TRs). We find that the selective basolateral expression of TRs is maintained in the face of extensive trafficking between the apical and basolateral surfaces. Biochemical studies of receptors loaded with tracer under conditions approaching steady state indicate that TRs internalized from the two surfaces are extensively colocalized within MDCK cells and that both populations of receptors are selectively delivered to the basolateral surface. Tailless TRs in which the cytoplasmic domain has been deleted display an unpolarized cell surface distribution and recycle in an unpolarized fashion. We show by EM that wild-type receptors internalized from each surface are

colocalized within endosomal elements distributed throughout the cytoplasm. By preloading endosomal elements directly accessible from the basolateral surface with transferrin (Tf)-HRP, we show that apically internalized TRs rapidly enter the same compartment. We also show that both transcytosing (apically internalized) and recycling (basolaterally internalized) TRs are delivered to the basolateral border by a distinctive subset of exocytotic, 60-nm-diam vesicles.

Together, the biochemical and morphological data show that apical and basolateral endosomes of MDCK cells are interconnected and contain a signal-dependent polarized sorting mechanism. We propose a dynamic model of polarized sorting in MDCK cells in which a single endosome-based, signal-dependent sorting step is sufficient to maintain the polarized phenotype.

T HE generation and maintenance of the polarized phenotype exhibited by epithelial cells have been studied intensively for two decades (Simons and Wandinger-Ness, 1990; Rodriguez-Boulan and Powell, 1992; Mostov et al., 1992). Pathways exist that can deliver newly synthesized proteins directly to either the apical or basolateral surface, and there are transcellular pathways which allow trafficking proteins to move across the polarized cell from one surface to the other. Sorting signals responsible for the basolateral delivery of many integral membrane proteins have been identified in their cytoplasmic tails (e.g., Aroeti et al., 1993; Matter et al., 1993), but the relationships between the biosynthetic pathways which deliver these proteins to the appropriate cell surface domain, the endocytic pathways which arise from these two domains and the transcytotic pathways which connect them, are ill-defined.

In MDCK cells, the most thoroughly characterized polarized system, there are biosynthetic routes that deliver membrane proteins to the apical and basolateral surfaces

directly, and the TGN has generally been postulated to be the primary site at which polarized sorting takes place (Simons and Wandinger-Ness, 1990; Matter and Mellman, 1994; Ikonen et al., 1995). The relationship between transcytotic and endocytic pathways has also been studied in these cells by following fluid-phase endocytosis (Bomsel et al., 1989; Parton et al., 1989). This work led to the suggestion that internalized proteins enter separate apical and basolateral endosomes and that there was an independent transcytotic pathway from each endosome to the opposite surface. However, more recent studies on polymeric IgA receptor trafficking in MDCK cells (Barroso and Sztul, 1994; Apodaca et al., 1994) have suggested that endosomal elements accessible from the basolateral border extend into the apical cytoplasm, where they may be directly accessible from the apical surface. Such an arrangement is similar to that described in polarized Caco-2 cells, where endosomal elements containing transferrin receptor (TR)[1] recycling from the basolateral border are accessible to membrane proteins recycling from the apical surface (Hughson and Hopkins, 1990; Knight et al., 1995).

Address all correspondence to Dr. Colin R. Hopkins, MRC Laboratory for Molecular Cell Biology, University College London, Gower Street, London WC1E 6BT England. Tel.: 0171-380 7806. Fax: 0171-380 7805.

---

1. *Abbreviations used in this paper:* RSV (A), Rous sarcoma virus subtype A; TR, transferrin receptor.

A polarized sorting mechanism within an endocytic pathway accessible from both surfaces would permit the continuous modulation of changing apical and basolateral distributions of trafficking membrane proteins caused by endocytosis and transcytosis and allow polarized sorting in the biosynthetic pathway to be much less stringent. Indeed, if newly synthesized proteins were delivered to the cell surface via an endosomal compartment capable of efficient polarized sorting, it would be unnecessary to postulate a separate polarized sorting mechanism at an earlier stage in the biosynthetic pathway (i.e., the TGN). Such pathways are known to exist because proteins such as the mannose-6-phosphate receptor and MHC class II–associated invariant chain (Kornfeld and Mellman, 1989; Odorizzi et al., 1994) are transferred directly from the Golgi complex to the endocytic pathway in fibroblasts and recent studies on epithelial cells have shown that a significant fraction of newly synthesized TRs and asialoglycoprotein receptors are also delivered to endosomes en route to the cell surface (Futter et al., 1995; Leitinger et al., 1995).

In the present study, we have expressed human TRs in MDCK cells and have followed the kinetics of TR internalization, recycling, and transcytosis from both surfaces. We show that wild-type TRs internalized from the basolateral border recycle back to the same surface with high efficiency, whereas those internalized from the apical surface are predominantly transcytosed to the basolateral border. Similar studies of tailless TRs demonstrate that this asymmetric routing depends upon a signal in the cytoplasmic domain. EM demonstrates that both recycling and transcytosing TRs become extensively colocalized within endosomal elements distributed throughout the apical cytoplasm and that a subset of 60-nm-diam vesicles derived from these elements carries both recycling and transcytosing TRs to the basolateral surface. We propose that a signal-dependent sorting mechanism is responsible for packaging TRs into these vesicles and suggest that this mechanism is sufficient to generate and maintain the polarized phenotype in MDCK cells.

Materials and Methods

Human TR Constructs

For construction of the wild-type TR-HRP chimera, a TR cDNA fragment encoding amino acids 1–119 (including the TR cytoplasmic and transmembrane domains plus the 30 membrane-proximal amino acids of the TR luminal domain) was generated by PCR using the wild-type TR cDNA as a template (McClelland et al., 1984), a 5′ oligo which places a ClaI restriction site 5′ of the TR initiation codon, and a 3′ oligo which places an ApaLI restriction site, a thrombin recognition sequence and glycine spacer (GALVPRGSPSGGGGGGGGG), and a BspEI restriction site 3′ of the TR Ala$_{119}$ codon. The HRP cDNA fragment was generated by PCR using the HRP isoenzyme c cDNA as a template (Amersham Corp., Arlington Heights, IL), a 5′ oligo which places a BspEI restriction site and the glycine spacer 5′ of the HRP cDNA sequence, and a 3′ oligo which places a stop codon and a ClaI restriction site 3′ of the HRP cDNA. The TR and HRP cDNA fragments were digested with BspEI and ligated. The tailless TR-HRP chimera was made by PCR using the TRΔ3-59 cDNA as a template (Jing et al., 1990). The resulting cDNA fragment was digested with ApaLI and ligated to the 3′ cDNA fragment of the TR-HRP chimera described above. ClaI fragments of the cDNAs encoding the wild-type and tailless TR-HRP chimeras, as well as of the cDNAs encoding the wild-type and tailless TRs, were cloned into RCAS-BP(A), a ret-

roviral expression vector derived from RSV(A) (Odorizzi and Trowbridge, 1994).

Expression of the RSV(A) Receptor in MDCK Cells

MDCK strain II cells (kindly provided by Ira Mellman, Yale University, New Haven, CT) were maintained in DMEM supplemented with 10% (vol/vol) defined bovine calf serum (Hyclone, Logan, UT). MDCK cells were transfected by calcium phosphate precipitation with pCB6(0.95), an expression plasmid encoding the 157–amino acid isoform of the RSV(A) receptor (Bates et al., 1993). After selection of transfected MDCK cells with 500 μg/ml geneticin (Gibco BRL, Gaithersburg, MD), individual clones which stably express the RSV(A) receptor were identified by Western blotting using antisera against the receptor (Bates et al., 1993).

Expression of Human TR Constructs in MDCK Cells

Transfection of CEF/O with recombinant RCAS-BP(A) retroviral constructs was performed as previously described (Odorizzi and Trowbridge, 1994). 2 wks after transfection, recombinant virus was concentrated by centrifugation of tissue culture supernatant at 23,000 rpm for 2.5 h at 4°C in a rotor (SW40 Ti; Beckman Instruments, Inc., Fullerton, CA), resuspended in 1 ml of DME, and passed through a 0.45-μm filter. A clone of MDCK cells that stably express the RSV(A) receptor were plated at 10^5 cells/well of a 24-well tissue culture dish (Costar Corp., Cambridge, MA), then incubated with concentrated recombinant virus for 12 h at 37°C. Afterward, the cells were grown to confluency in growth medium. Expression of TRs was analyzed by immunofluorescence using B3/25, an mAb against the extracellular domain of the receptor, and a goat anti–mouse secondary antibody conjugated to FITC (Cooper Biomedical, Malvern, PA). Expression of TR-HRP chimeras was analyzed by immunofluorescence using an anti-HRP antibody conjugated to FITC (Cooper Biomedical). Individual clones of MDCK cells expressing human TRs and TR-HRP chimeras were isolated by limited dilution, and the polarity of clones was verified both by measuring the transepithelial electrical resistance and by monitoring the secretion of gp80 into the apical medium (Urban et al., 1987). Immunoprecipitation from MDCK cells of human TRs with either H68, a mAb against the human TR cytoplasmic domain (White et al., 1992) which cross-reacts with canine TRs, or B3/25, which is human specific, indicated that human TRs did not form mixed dimers with endogenous canine TRs (data not shown).

Steady-State Surface Distributions of Human TRs in MDCK Cells

MDCK cells expressing wild-type or tailless TRs were seeded at high density onto 24-mm-diam polycarbonate filters (0.4 μm pore size) (Transwell; Costar Corp.) and cultured for 3 d, with the media changed every other day. ^{125}I-labeled diferric human Tf (ICN Biomedicals, Irvine, CA) was prepared by incubating 500 μg Tf with 40 μg chloramine T (Sigma Chemical Co., St. Louis, MO) and 0.5–1.0 mCi Na^{125}I (Amersham Corp.) in a total vol of 150 μl of PBS. The reaction was stopped by adding 80 μg sodium metabisulfite (Fisher Scientific, Fair Lawn, NJ) in 10 μl of PBS. ^{125}I-labeled Tf was separated from free ^{125}I on a Sephadex G-25 column equilibrated in PBS. For experimentation, cells were incubated in DME for 1 h at 37°C, then shifted to 4°C and washed with 0.5% BSA-PBS$^+$ (PBS with 1 mM CaCl$_2$ and 1 mM MgCl$_2$) (BSA-PBS$^+$). Cells were then incubated for 1 h at 4°C with 4 μg/ml ^{125}I-labeled Tf in BSA-PBS$^+$ added to either side of the monolayer. Less than 0.1% of the ^{125}I-labeled Tf diffused through the monolayers. Cells were then washed three times at 4°C with BSA-PBS$^+$, and the amount of radioactivity specifically bound was determined by excising the filters and counting them in a gamma counter. Control MDCK cells bound <10% of the amount of Tf bound by MDCK cells expressing human TRs. Wild-type TRs were found to have a >90% basolateral steady-state surface distribution in four individual cell clones which expressed ∼50,000–200,000 total cell surface receptors (data not shown). These clones were used in subsequent experiments which measured endocytosis and recycling of wild-type TR.

MDCK monolayers expressing wild-type or tailless TR-HRP chimeras were washed three times with TBS (10 mM Tris-HCl, pH 7.5, 150 mM NaCl, 2.5 mM CaCl$_2$, 1 mM MgCl$_2$) and cooled to 4°C. The apical and basolateral sides of the monolayers were then incubated in 100 μl of 50 U/ml human thrombin (Sigma Chemical Co.) in TBS at 4°C for 30 min. Afterward, 70 μl was removed from each side and added to 250 μl of 2,2′-Azino-di-[3-ethylbenzthiazolinesulfonate] (ABTS) (Boehringer-Mann-

heim Biochemicals, Indianapolis, IN), and the absorbance of the reaction product was measured at 405 nm.

Biosynthetic Transport of Human TRs to the Surface of MDCK Cells

MDCK monolayers expressing wild-type or tailless TRs were incubated for 30 min at 37°C in methionine- and cysteine-free DME containing 0.5 mCi/ml trans-^{35}S-label (ICN Biomedicals) and 1% dialyzed fetal bovine calf serum. Monolayers were then washed three times with DME and chased for 20 or 40 min in DME at 37°C. The cells were then chilled with two washes in DME at 4°C, and either the apical or basolateral surface was incubated for 30 min in DME containing 100 μg/ml trypsin (Worthington Biochemical Corp., Freehold, NJ). DME containing 100 μg/ml trypsin inhibitor (Sigma Chemical Co.) was added to the opposing surface. TR extracellular domain fragments were then immunoprecipitated from the apical and basolateral media using B3/25 mAb and analyzed on 10% SDS polyacrylamide gels. Dried gels were exposed to preflashed XAR film (Eastman Kodak, Rochester, NY), and quantitation of radioactivity was performed on a model 425 PhosphorImager (Molecular Dynamics, Sunnyvale, CA).

Endocytosis of Human TRs from the Apical and Basolateral Surfaces of MDCK Cells

To measure the rates of endocytosis of TRs, monolayers were incubated for 1 h at 37°C in DME, then shifted to 4°C and washed once with 0.5% BSA-DME (BSA-DME). Cells were then incubated for 1 h at 4°C with 4 μg/ml ^{125}I-labeled Tf in BSA-DME added either apically or basolaterally. Unbound Tf was removed with three washes at 4°C in BSA-DME. Cells were then incubated at 37°C for various periods of time in BSA-DME. The monolayers were subsequently washed twice at 4°C with BSA-PBS$^+$, the filters were excised, and surface-bound and internalized Tf were distinguished using an acid wash procedure (Hopkins and Trowbridge, 1983). To facilitate the measurement of endocytosis from the apical border, the number of receptors at this surface was increased by incubating monolayers in 10 mM sodium butyrate for 12–16 h before experimentation (Gottlieb et al., 1986a).

To measure the kinetics with which the internal distributions of apically and basolaterally endocytosed TRs achieve equilibrium, monolayers were incubated for 1 h at 37°C in DME, then incubated for various periods of time at 37°C with 10 μg/ml ^{125}I-labeled Tf in BSA-DME added to either side. Cells were then washed three times at 4°C with BSA-PBS$^+$ to remove unbound Tf, and the filters were excised. Surface-bound Tf was removed with an acid wash (Hopkins and Trowbridge, 1983), and the remaining cell-associated radioactivity was measured.

Colocalization of Human TRs Endocytosed from the Apical and Basolateral Surfaces of MDCK Cells

Monolayers expressing wild-type TRs were incubated for 1 h at 37°C in DME then for 2 h at 37°C in BSA-DME with ^{125}I-labeled Tf (1–4 μg/ml) added to the basolateral medium, and B3/25-HRP conjugate (500 μg/ml) added to either the basolateral or apical medium. Under these conditions, <20% of TRs loaded apically with B3/25-HRP would be expected to have been transcytosed to the basolateral border and re-internalized (see Fig. 5). Cells were then washed three times at 4°C with TS (50 mM Tris, pH 7.6, 0.9% NaCl). Cross-linking was performed by incubating cells for 30 min at 4°C in TS containing 100 μg/ml DAB (Aldrich Chemical Co., Milwaukee, WI) and 0.06% H$_2$O$_2$. Monolayers were then washed three times at 4°C with TS, the filters were excised, and the cells were lysed in TS containing 1% Triton X-100 and 15 mM NaN$_3$ for 10 min at 4°C. Lysates were centrifuged at 14,000 rpm for 15 min at 4°C, and the radioactivity in the supernatants was determined. Insoluble complexes were measured as the radioactivity in the pellets plus the radioactivity remaining associated with the filters. The percentages of insoluble complexes were determined from the total radioactivity recovered in the soluble and insoluble fractions.

Recycling and Transcytosis of Human TRs in MDCK Cells

To measure the recycling of wild-type and tailless TRs internalized from the apical or basolateral surfaces, monolayers were incubated for 1 h at 37°C in DME then for 30 min at 37°C with 4 μg/ml ^{125}I-labeled Tf in BSA-DME added to either side. Cells were then washed three times at 4°C with

BSA-DME, and surface-bound Tf was removed with >95% efficiency using deferoxamine mesylate as previously described (Jing et al., 1990). Cells were then washed three times with BSA-DME and incubated at 37°C for 60 min in BSA-DME containing 100 μg/ml unlabeled Tf. Afterward, the radioactivity released into the apical and basolateral media, as well as the cell-associated radioactivity, was determined. Radioactivity collected from control MDCK cells was ~12 and ~34% of the amounts collected from cells expressing the human wild-type and tailless TRs, respectively, and was subtracted. Cells growing on the Transwell chamber wall were lysed with 1 M NaOH after removal of the filter, and the radioactivity in the lysate was measured. Radioactivity released from these cells was estimated to be ~15% of the total radioactivity collected in the apical media after reculture at 37°C and was subtracted from the total.

To measure the kinetics with which a single cohort of wild-type TRs are transcytosed, monolayers were loaded with ^{125}I-labeled Tf either apically or basolaterally as described above for 5 min at 37°C. After removal of surface-bound Tf at 4°C with deferoxamine mesylate, monolayers were incubated at 37°C for various periods of time, and the radioactivity was collected as described above.

To measure the rate of transcytosis of TRs, monolayers were incubated first with DME for 1 h at 37°C, then incubated with ^{125}I-labeled Tf in 0.5% BSA-DME added either apically or basolaterally at 37°C for various periods of time. Afterward, the appearance of ^{125}I-labeled Tf in the opposing media was monitored, and the surface and internal distributions of the cell-associated ^{125}I-labeled Tf were determined as described above using the acid wash procedure.

Electron Microscopy

Tf-HRP and B3/25-HRP were prepared by conjugating 10 mg of Tf or B3/25 mAb to 10 mg of HRP (type II; Sigma Chemical Co.) using SPDP as previously described (Hopkins, 1985). Free HRP was removed from the conjugate using the FreeZyme conjugate purification kit (Pierce, Rockford, IL). 5–8 nm colloidal gold sols were made as described by Slot and Geuze (1985). B3/25 mAb was complexed to colloidal gold as described previously (Hopkins, 1985). Before incubation, gold complexes were washed by centrifugaton in an airfuge (Beckman Instruments, Inc.) at 150,000 g for 5 min.

For electron microscopy, cells were fixed in dilute Karnovsky fixative (2% paraformaldehyde, 2.5% glutaraldelyde in 0.1M Na cacodylate buffer, pH 7.5) (Karnovsky, 1965), postfixed in reduced osmium tetroxide, and embedded in Epon as described previously (Hopkins and Trowbridge, 1983). Sections were either cut at 70 nm and stained with uranyl acetate and lead citrate or cut up to 1.0 μm thick, stabilized with a thin film of evaporated carbon, and viewed unstained, in an electron microscope (CM12; Philips Electronic Instruments Co., Mahwah, NJ). To increase the detection of TRs morphologically, monolayers were incubated in 10 mM sodium butyrate 12–16 h at 37°C before experimentation (Gottlieb et al., 1986a). Identical results were obtained in experiments performed without the inclusion of sodium butyrate.

To clear the biosynthetic pathway of newly synthesized TR-HRP chimeras, monolayers were incubated for 2 h in medium containing 1 mM DTT (Stinchcombe et al., 1995).

Quantitation of 60-nm-diam vesicles containing Tf-HRP endocytosed from either surface was made on sections of cells in which the full longitudinal axis of the cell was displayed. As shown in Fig. 9 a, a line was drawn at the level of the junctional complexes to delineate the apical and basolateral cytoplasm, and the areas of cytoplasm within these domains were estimated using point and intersection counting (Weibel, 1979). Micrographs with a magnification of 10,000 were overlaid with a square lattice grid of 5 mm and the number of vesicles with a diameter between 40 and 60 nm that were Tf-HRP positive were counted and normalized for cytoplasmic areas (1,646–1,913 mm^2). Although the number of vesicles varied with levels of expression up to threefold, the relative percentages of vesicles present in the cytoplasm at the apical and basolateral borders was consistent and varied by <5%.

Results

The Cytoplasmic Domain Directs TRs and TR-HRP Chimeras to the Basolateral Surface of MDCK Cells

Human TRs and TR-HRP chimeras, in which the luminal domain of TR is replaced by HRP, were stably expressed

in MDCK cells by infection with a Rous sarcoma virus subtype A (RSV(A)) retroviral vector. The RSV(A) cell surface receptor (Bates et al., 1993) had been expressed in the MDCK cells, rendering them competent for infection by RSV(A) (see Materials and Methods). ^{125}I-labeled Tf-binding studies showed that >90% of the surface wild-type TRs were distributed on the basolateral border at steady state, whereas the distribution of tailless TRs was essentially random (Fig. 1 A). The influence of the cytoplasmic domain on the polarized distribution of TRs was also monitored by analysis of TR-HRP chimeras containing a thrombin cleavage site between the TR and HRP sequences. The surface distributions of the chimeras were measured by quantitating the HRP activity released from either surface of the monolayer when incubated in thrombin-containing medium. Monolayers which express wild-type TR-HRP chimeras (which bear the TR cytoplasmic tail) displayed ~90% of the thrombin-cleavable HRP at the basolateral surface (Fig. 1 B), identical to the distribution of wild-type TRs. Conversely, tailless TR-HRP chimeras had an essentially random surface distribution. Thus, the TR-HRP chimeras are targeted by a sorting signal in the TR cytoplasmic tail and accurately reflect the distributions of TRs in MDCK cells. As shown in Fig. 1 C, newly synthesized TRs are also subjected to signal-dependent sorting to the basolateral surface, as >90% of wild-type TRs are delivered to the basolateral surface, whereas the tailless receptor is delivered to both surfaces in approximately equal amounts. These results demonstrate that the polarized basolateral distribution of TRs in MDCK cells requires the cytoplasmic domain of the receptor and that the removal of this domain alone results in an unpolarized surface distribution.

TRs on the Apical and Basolateral Surfaces of MDCK Cells Belong to Common Pool

In pulse-chase experiments using ^{125}I-labeled Tf, wild-type TRs were rapidly internalized from both the basolateral and apical surfaces, although the rate of internalization from the basolateral surface was two to three fold faster (Fig. 2 A). A similar difference in kinetics of internalization of a mutant influenza hemagglutinin from the apical and basolateral surfaces of MDCK cells has recently been described and was determined to be the result of slower coated pit maturation at the apical domain (Naim et al., 1995). As expected, MDCK cells expressing tailless TRs poorly internalized Tf from both surfaces, displaying a relative internalization efficiency of ~10% that of wild-type TRs (data not shown).

Continuous incubation with ^{125}I-labeled Tf in the apical medium resulted in a gradual accumulation of radiolabel in the intracellular pool for at least 2 h (Fig. 2 B). In contrast, continuous basolateral incubation with ^{125}I-labeled Tf resulted in an initial peak of intracellular tracer at 10 min followed by a ~30% decline to equilibrium by 1 h (Fig. 2 B). As a result, the intracellular accumulation of ^{125}I-labeled Tf loaded for 2 h from the apical surface was similar to that loaded from the basolateral surface despite the fact that only ~10% of the total cell surface TRs are displayed on the apical surface at steady state (Fig. 1). Experiments in which continuous incubation with ^{125}I-labeled
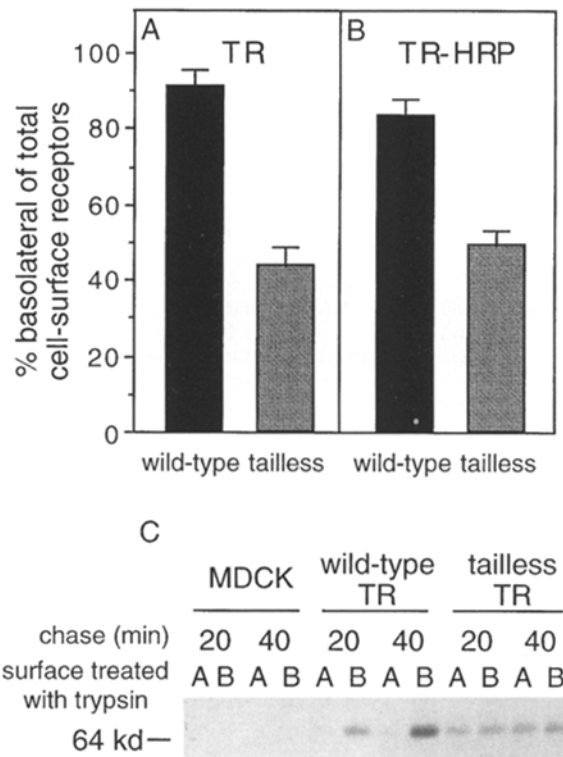
Figure 1. Removal of the TR cytoplasmic tail results in the non-polarized cell surface expression of TR and TR-HRP chimeras. (A) The amount of ^{125}I-labeled Tf specifically bound at 4°C to the apical or basolateral surface of MDCK monolayers expressing wild-type or tailless TRs was determined. The values shown represent 38 (wild-type) or 8 (tailless) independent experiments performed with four or three individual clones, respectively. (B) The apical or basolateral surfaces of monolayers expressing wild-type or tailless TR-HRP chimeras were incubated at 4°C for 30 min with human thrombin (50 U/ml). Release of HRP moieties of surface chimeras into the surrounding medium was measured as described in Materials and Methods. The values shown represent 51 (wild-type) or 9 (tailless) independent experiments performed with one or four individual clones, respectively. (C) Newly synthesized wild-type or tailless TRs were labeled with trans-^{35}S-label for 30 min and chased to the cell surface for 20 or 40 min at 37°C. Receptors at the apical (A) or basolateral (B) surface were then cleaved at 4°C for 30 min with trypsin (100 μg/ml). Trypsin inhibitor (100 μg/ml) was included in the opposing media. B3/25 mAb immunoprecipitates of the TR extracellular fragments in the media collected from each surface were analyzed on SDS polyacrylamide gels and quantitated by phosphorimage analysis. No material could be detected in immunoprecipitates from the media containing trypsin inhibitor.

Tf was extended to 4 h confirmed that the intracellular pool of TRs was labeled at least as efficiently from the apical surface as from the basolateral surface as equilibrium was approached (data not shown). At equilibrium, however, a complicated balance exists in which a significant fraction of intracellular TRs initially loaded with ^{125}I-labeled Tf from one surface will have transcytosed to the opposite surface and released their ligand into the medium (see Fig. 5). These will remain unlabeled until they return to the original surface. Consequently, the initial peak followed by a decline in intracellular ^{125}I-labeled Tf loaded

142
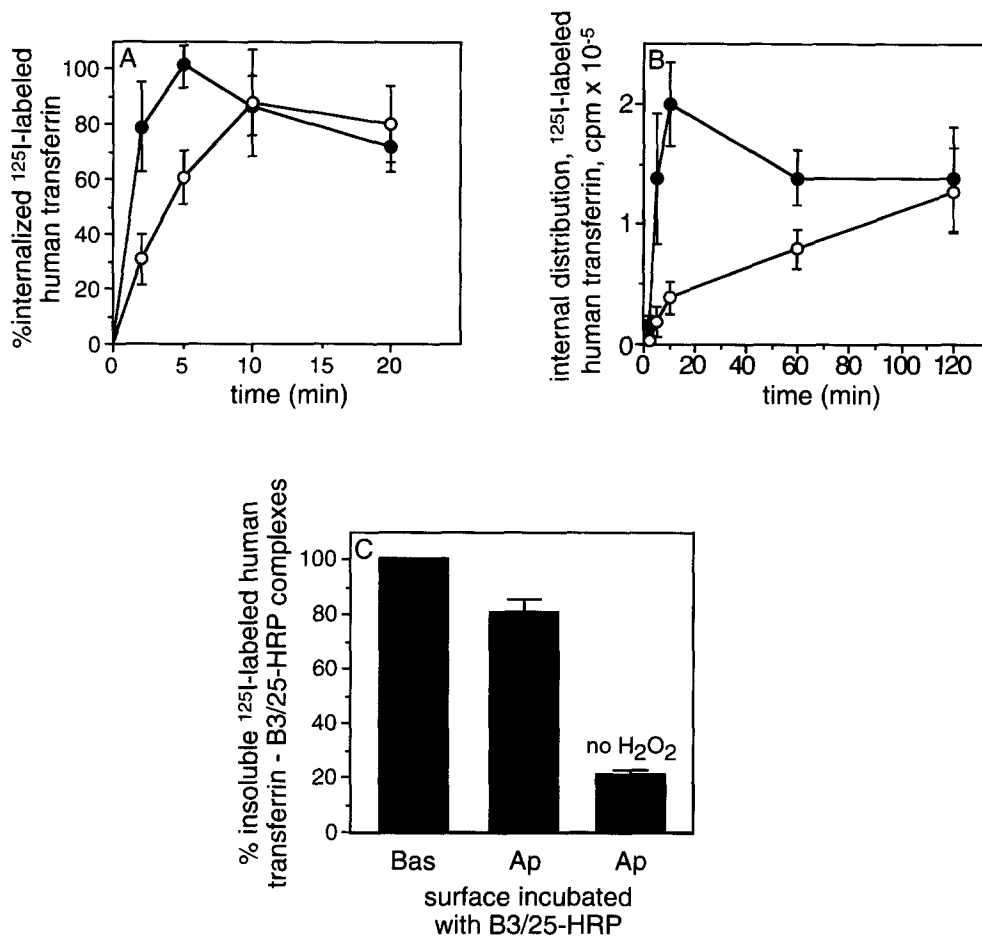
Figure 2. TRs on the apical and basolateral surfaces of MDCK cells belong to a common pool. (*A*) Monolayers expressing wild-type TRs were incubated for 1 h at 4°C with ^{125}I-labeled Tf added to either the apical (*open circles*) or basolateral (*closed circles*) surface. Unbound Tf was removed, and monolayers were incubated at 37°C in BSA-DME for various periods of time. Monolayers were then chilled to 4°C, and surface bound and internalized Tf were determined using an acid wash procedure. (*B*) ^{125}I-labeled Tf was added for various periods of time at 37°C to either the apical (*open circles*) or basolateral (*closed circles*) surface of monolayers expressing wild-type TRs. Cells were then chilled to 4°C, and surface bound and internalized Tf were determined. (*C*) ^{125}I-labeled Tf was added to the basolateral medium of monolayers expressing wild-type TRs for 2 h at 37°C, with B3/25-HRP (500 µg/ml) included in either the basolateral or apical medium. Cross-linking was performed with DAB +/− H₂O₂ at 4°C, and insoluble complexes from Triton X-100 lysates were harvested by centrifugation. Results are expressed as the percentage of insoluble radioactivity relative to the percentage of insoluble radioactivity obtained from cells incubated with both ^{125}I-labeled Tf and B3/25-HRP added to the basolateral surface.

from the basolateral surface most likely reflects the initial rapid filling of the intracellular compartment with radiolabel followed by dissociation of the radiolabel from the cohort of receptors transcytosed to the apical surface and the fact that the fraction of transcytosed and empty TRs increases until a constant rate of basolateral-to-apical transcytosis is achieved after 20–40 min of continuous loading (see Fig. 5).

The extent to which apically and basolaterally endocytosed TRs traffic along common intracellular pathways was measured by loading monolayers at 37°C for 2 h with ^{125}I-labeled Tf from the basolateral surface and B3/25 (anti-TR mAb)-HRP conjugate from the apical surface. Colocalized tracers were then cross-linked at 4°C using diaminobenzidine, forming insoluble complexes which were harvested by centrifugation from cells lysed in Triton X-100. Compared with the maximum amount of radiolabeled Tf cross-linked when monolayers were loaded with both tracers basolaterally, ~80% of basolaterally loaded Tf could be cross-linked by apically loaded B3/25-HRP (Fig. 2 *c*). Since the protocol used ensures that receptors loaded with either tracer are unlikely to have an opportunity to reinternalize (see Fig. 5), and in the case of Tf will dissociate on reaching the apical surface, this extensive cross-linking shows that most

TRs endocytosed from the apical surface must traffic through compartments containing TRs internalized from the basolateral surface.

TRs Endocytosed from the Apical and Basolateral Surfaces of MDCK Cells Are Predominantly Recycled to the Basolateral Surface

The recycling of Tf internalized from either the apical or basolateral border was measured independently of internalization or direct dissociation of Tf from surface receptors by loading the endocytic pathway of MDCK monolayers with ^{125}I-labeled Tf applied to either the apical or basolateral surface for 30 min at 37°C, then cooling the cells to 4°C before removing surface-bound Tf with deferoxamine mesylate (see Materials and Methods). Monolayers containing internalized ^{125}I-labeled Tf were then incubated at 37°C, and the appearance of radioactivity in the apical and basolateral media was monitored.

As shown in Fig. 3 *A*, cells expressing wild-type TRs which were loaded with ^{125}I-labeled Tf from the basolateral border selectively recycled >80% of the Tf back to this surface. Remarkably, this polarity was maintained when Tf was internalized from the apical surface, as api-
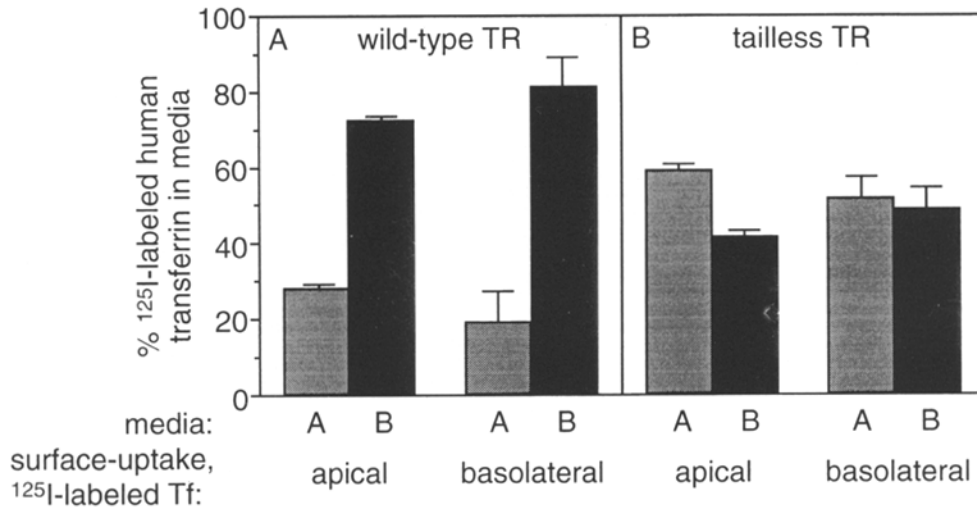
Figure 3. Wild-type TRs internalized from the apical and basolateral surfaces of MDCK cells recycle predominantly to the basolateral border. Monolayers expressing wild-type (*A*) or tailless (*B*) TRs were incubated at 37°C for 30 min with ^{125}I-labeled Tf added to either the apical or basolateral surface. Cells were then washed, and surface-bound ^{125}I-labeled Tf was removed at 4°C with deferoxamine mesylate. Monolayers were then incubated at 37°C for 60 min, and the appearance of ^{125}I-labeled Tf in the apical (■) and basolateral (■) media was determined. More than 90% of the internalized ^{125}I-labeled Tf recycled after 60 min at 37°C.

cally loaded cells released >70% of their Tf into the basolateral medium (Fig. 3 *A*). TRs were recycled with the same degree of polarity to the basolateral surface when loaded for 120 min from either surface (data not shown). Thus, wild-type TRs are predominantly delivered to the basolateral border regardless of the surface from which they are endocytosed. Conversely, when cells expressing tailless TRs were loaded with ^{125}I-labeled Tf from either the apical or basolateral surface, Tf was recycled without polarity (Fig. 3 *B*), indicating that the TR cytoplasmic tail is required to maintain the asymmetric delivery of TRs to the basolateral border following endocytosis from either surface domain.

To examine the kinetics of recycling and transcytosis of TRs in MDCK cells, ^{125}I-labeled Tf was loaded for 5 min at 37°C from either the apical or basolateral surface before removal of surface-bound Tf at 4°C with deferoxamine mesylate. The cells were then incubated at 37°C for various periods of time, and the ^{125}I-labeled Tf released into the apical and basolateral media, as well as the cell-associated radiolabel, was monitored. As shown in Fig. 4, *A* and *C*, this pulse-chase protocol revealed an additional feature of the trafficking of TRs internalized from the apical surface. Unlike receptors loaded apically with ^{125}I-labeled Tf for 30 min (Fig. 3 *A*), the cohort of TRs labeled from the apical surface during the 5-min pulse was not predominantly routed to the basolateral surface. Instead, ~60% of the ^{125}I-labeled Tf released from the cells after 90 min was recycled to the apical medium, and ~40% was transcytosed to the basolateral medium (Fig. 4 *C*). This distribution resulted from two competing processes that direct the movement of apically internalized TRs: rapid recycling of receptors to the apical surface versus slower transcytosis of TRs to the basolateral surface. Recycling of apically internalized Tf occurred with a half-time of ~10 min, whereas transcytosis occurred more than twofold slower (Fig. 4 *A*). The marked difference between the rates of recycling and transcytosis is most evident in Fig. 4 *C*, which shows that

>90% of the ^{125}I-labeled Tf released from the cells after 5 min of chase was in the apical medium. The data in Fig. 3 *A* and Fig. 4, *A* and *C* imply that when receptors carrying ^{125}I-labeled Tf enter the endosomal compartment proximal to the apical surface, the majority recycle apically, but as the radiolabel becomes more widely distributed throughout the endosome, recruitment to transcytotic pathways becomes increasingly significant. After 30 min, when the endosome compartment has become sufficiently filled with ^{125}I-labeled Tf, the basolateral route predominates, and up to 70% of the apically internalized tracer is trancytosed. Transcytosis of ~40% of TRs in cells loaded for only 5 min suggests, however, that recycling predominates over transcytosis in only the most proximal elements of the endosomal compartment accessible from the apical surface.

In contrast to apically loaded TRs, the cohort of receptors pulse-labeled from the basolateral surface for 5 min was recycled back to the basolateral surface with the same high selectivity as TRs loaded for 30 min (compare Fig. 4, *B* and *D* with Fig. 3 *A*). Thus, the polarized sorting machinery that selectively recycles wild-type TRs to the basolateral surface appears to be located within the most peripheral elements of the endosomal compartment accessible from the basolateral surface.

Together, these results imply that maintenance of the polarized cell surface phenotype displayed by the wild-type TR in MDCK cells is a highly dynamic process involving repeated rounds of internalization and selective sorting of receptors trafficking along the endocytic pathway back to the basolateral surface. To quantitate the trafficking of TRs between the apical and basolateral surfaces of MDCK cells, ^{125}I-labeled Tf was continuously loaded from either the basolateral or apical surface, and the release of radiolabel into the opposing medium was monitored. Significant amounts of ^{125}I-labeled Tf were transcytosed from the apical to the basolateral surface only after 40 min, and the rate of apical-to-basolateral transcytosis only began to equal the rate of basolateral-to-apical trans-
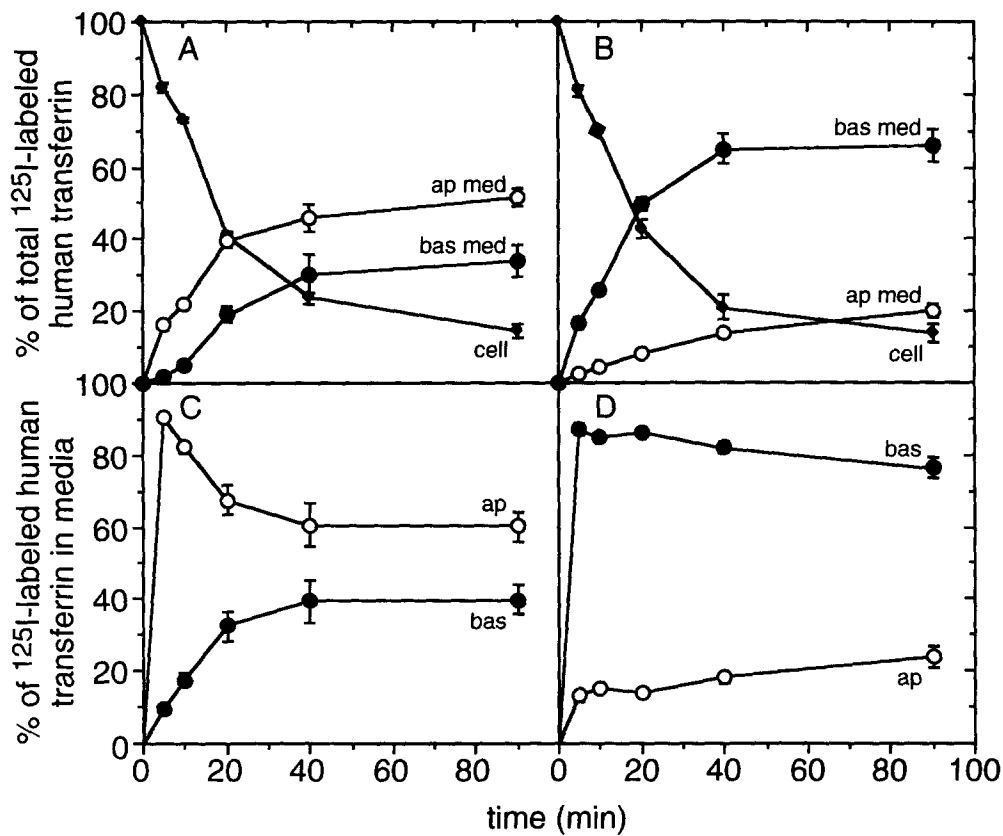
Figure 4. Kinetics of recycling and transcytosis of TRs endocytosed from the apical and basolateral surfaces of MDCK cells. Monolayers expressing wild-type TRs were incubated at 37°C for 5 min with ^{125}I-labeled Tf added to either the apical (*A* and *C*) or basolateral (*B* and *D*) surface. Cells were then washed, and surface-bound ^{125}I-labeled Tf was removed at 4°C with deferoxamine mesylate. Monolayers were then incubated at 37°C for various periods of time, and the appearance of ^{125}I-labeled Tf in the apical (*open circles*) or basolateral (*closed circles*) media, as well as the remaining cell-associated radioactivity (*closed diamonds*), was monitored.

cytosis after 2 h (Fig. 5). These results reflect the slower kinetics with which apically loaded Tf fills the intracellular pool (Fig. 2 *B*) and is transcytosed (Fig. 4). The extensive flux of TRs between the apical and basolateral surfaces of MDCK cells can be appreciated by expressing the ^{125}I-labeled Tf transcytosed in both directions at equilibrium in terms of the number of receptors expressed on each surface. Thus, an amount equivalent to half of the basolateral surface population of TRs crosses the apical surface per hour, whereas an amount equivalent to three to fourfold of the apical surface population of TRs crosses the basolateral surface per hour. These values are consistent with the selective delivery of internalized TRs to the basolateral surface regardless of the surface from which they are endocytosed.

TRs Endocytosed from the Apical and Basolateral Surfaces of MDCK Cells Become Extensively Colocalized

For morphological studies Tf-HRP conjugates and B3/25–gold complexes were used as tracers to delineate the endocytic pathways from both the apical and basolateral surfaces. With Tf-HRP applied basolaterally and B3/25-gold applied apically for 60 min at 37°C, the majority of endosomal tubules and vesicles were labeled with both tracers (Fig. 6 *a*). The same result was obtained with B3/25–gold applied basolaterally and Tf-HRP applied apically (Fig. 6 *b*) and could be achieved with incubations as short as 15 min (data not shown). Together, the vacuolar and tubular elements labeled with both tracers identify widely distrib-

uted endosomal elements accessible to TRs internalized from both the apical surface and the basolateral surface. The routes from both surfaces include clathrin-coated pits, 0.3–0.5 μm diameter vacuoles, and a variety of tubules and vesicles which extend from below the basolateral surface to the apical cytoplasm. The vacuoles are distinctive be-
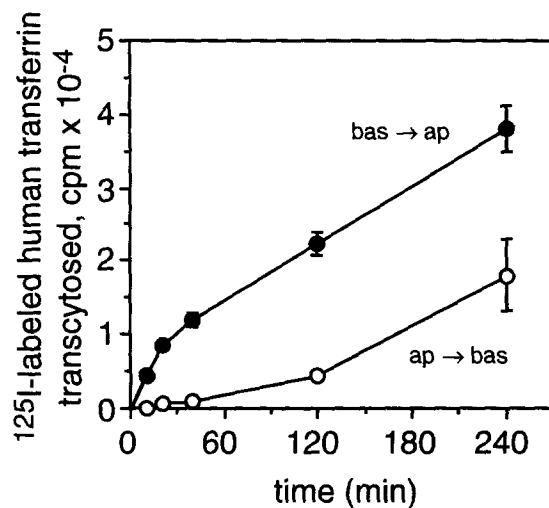
Figure 5. TRs traffic extensively between the apical and basolateral surfaces of MDCK cells. Monolayers expressing wild-type TRs were incubated either apically (*open circles*) or basolaterally (*closed circles*) with ^{125}I-labeled Tf at 37°C for various periods of time, and the appearance of radioactivity in the opposing medium was monitored.

cause only a small proportion of them are typical multivesicular endosomes or lysosomes (Fig. 6, *a* and *b*). The majority does not contain internal vesicles, and in section planes that are equatorial rather than tangential, it is clear that the HRP and gold TR tracers are closely associated with their perimeter membranes. Lysosomes (Fig. 6 *b*) contain very little gold or HRP tracer. Two distinct size classes of tubules and vesicles were labeled. The larger form is between 100 and 250 nm in diameter (Fig. 6 and Fig. 7), whereas the smaller form has a more constant diameter of 55–60 nm (Fig. 7 *c*). The proportion of Tf-HRP–labeled vesicles with a diameter of <60 nm distributed within the apical and basolateral cytoplasm was quantitated morpho-metrically by drawing a line across micrographs at the level of the junctional complexes on cells in which the full longitudinal axis was displayed. When Tf-HRP was loaded from either the apical or basolateral border, ~85% of the total labeled vesicle population was located in the basolateral cytoplasm (Fig. 8). However, after 1 h at 37°C, five times more labeled vesicles were in the basolateral cytoplasm when a monolayer was loaded from the basolateral surface compared to loading from the apical surface. Thus, even after 1 h of continuous incubation, tracers loaded from the apical surface gain access to only a proportion of the basolateral 60-nm-diam vesicle population. This observation is consistent with the kinetic data shown in Fig. 2 *B*
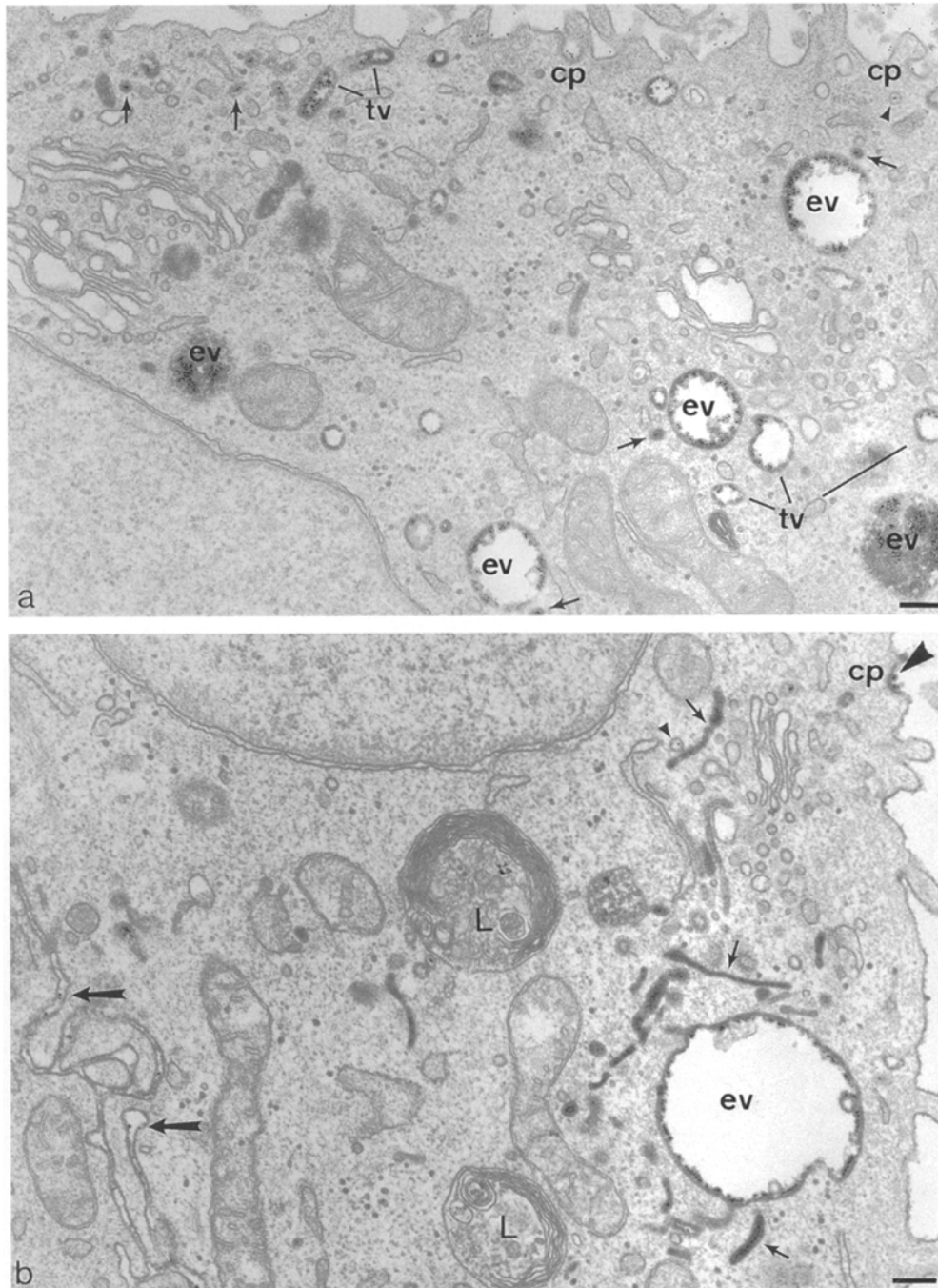
Figure 6. Endosome vacuoles and tubules are labeled simultaneously from both the apical and basolateral surfaces. Monolayers expressing wild-type TRs were incubated for 60 min at 37°C with (*a*) Tf-HRP in the basolateral medium and B3/25-gold in the apical medium, or (*b*) B3/25-gold in the basolateral medium and Tf-HRP in the apical medium. Elements containing both tracers include endosomal vesicles (*ev*), 250-nm-diam tubulo vesicles (*tv*) and 60-nm-diam tubules and vesicles containing both tracers (*small arrows*) or only B3/25-gold (*small arrowheads*). Coated pits on the apical membrane contain concentrated tracer. In *b*, it is evident that gold tracer has transcytosed from the basolateral surface (*large arrows*) to the apical surface (*large arrowhead*). *L*, lysosome. Bar, 0.2 μm.
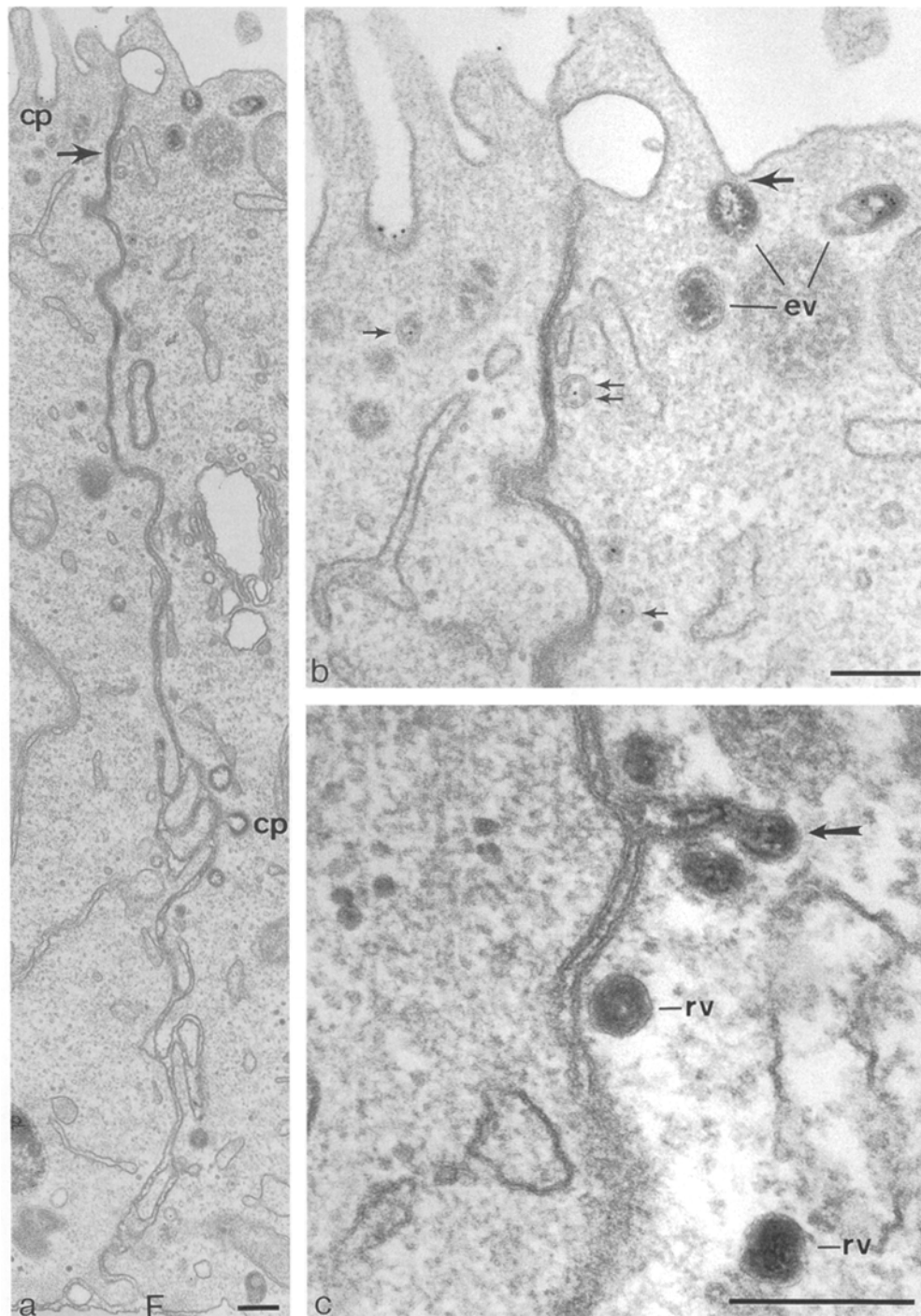
Figure 7. 60-nm-diam vesicles contain both transcytosing and recycling TRs. Monolayers expressing wild-type TRs were incubated for 60 min at 37°C with Tf-HRP added basolaterally and B3/25-gold added apically. (*a*) Low power view of the basolateral border from the junctional area (*large arrow*) to the filter (*F*), showing the distributions of apical and basolateral coated pits (*cp*). (*b*) Detail from the apical region of *a* to show 60-nm-diam vesicles containing recycling Tf-HRP and apically derived gold tracer (*small arrows*) and endosomal tubulo vesicles displaying basolaterally derived Tf-HRP at their perimeter membrane (*ev*). Double arrows indicate a transcytotic vesicle which is clearly labeled with both tracers. Note the close proximity to the apical membrane of the endosomal tubulo vesicles containing basolaterally derived tracer (*large arrow*). (*c*) Distribution of peroxidase reaction product in recycling 60-nm-diam vesicles (*rv*) lying adjacent to the basolateral border. Note exocytic profile (*arrow*) and absence of cytoplasmic coats on these exocytic vesicles. Bar, 0.2 μm.

and Fig. 5, showing that maximal uptake and transcytosis of ^{125}I-labeled Tf in the apical-to-basolateral direction is only achieved after 2 h. It also suggests that basolateral exocytotic vesicles would be one of the last compartments to be fully penetrated by receptors loaded from the apical surface.

The kinetics with which the basolaterally distributed 60-nm-diam vesicles became labeled with apically derived tracer was followed in monolayers loaded to equilibrium from the basolateral surface with Tf-HRP and then incubated apically with B3/25–gold (Fig. 9). When B3/25-gold was applied as a pulse (incubated at 5°C for 1 h before

transfer to 37°C), it was contained within Tf-HRP–positive endosomal elements within 5 min of the warm up from 5°C (Fig. 9). Internalized tracer was not observed before this 5-min time point and at this time the only elements which contained only gold were 60–80-diam vesicles which are probably clathrin-coated vesicles that have become uncoated. Intermediate endosomal elements containing only gold tracer were not observed, and we conclude, therefore, that vesicles containing TRs derived from coated pits on the apical plasma membrane fuse directly with endosomes containing basolaterally applied Tf-HRP. As demonstrated for ^{125}I-labeled Tf (Fig. 5), basolaterally applied Tf-HRP
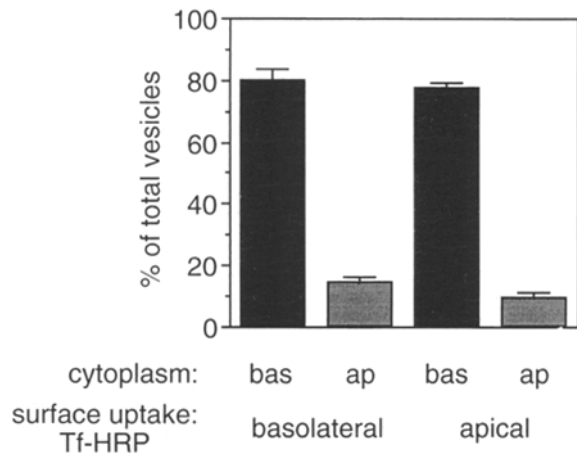
Figure 8. Quantitation of 60-nm-diam vesicles containing Tf-HRP. Monolayers loaded with Tf-HRP from either the apical or basolateral surface were embedded and sectioned to display the long axis of the cell. A line was drawn to connect the junctional complexes (see Fig. 10) and the number of 60-nm-diam vesicles containing Tf distributed in the apical and basolateral cytoplasm was quantitated morphometrically (see Materials and Methods). >80% of the vesicles are basolateral regardless of which side of the monolayer the Tf-HRP is internalized.

would be expected to be released into the medium upon reaching the apical surface, and in general, basolaterally applied Tf-HRP is not seen on the apical surface (Fig. 6 *a* and Fig. 7 *b*). Tf-HRP found in endosomes below the apical surface is thus unlikely to be tracer reinternalized from the apical surface.

Most endosomal structures became labeled with apically internalized tracer within 10 min. The 60-nm-diam vesicles, however, contained both apically and basolaterally internalized tracers only after incubations of 10 min or longer, at the time when apically internalized B3/25–gold first became detectable in the intercellular space at the basolateral border. Direct counting of labeled vesicles showed that after 5 min, <5% of the basolateral Tf-HRP–positive 60-nm-diam vesicles contained apically internalized tracer, whereas after 30 min, 47% of these vesicles contained both tracers. The delay in the appearance of apically internalized B3/25–gold within these vesicles

clearly indicates that they lie at the distal end of the apical-to-basolateral transcytotic pathway.

The interrelationships between the various TR-containing elements were strikingly displayed in monolayers that express wild-type TR-HRP chimeras. In these cells, peroxidase activity was detectable throughout the biosynthetic pathway and in all of the endocytic elements which could be labeled by externally applied Tf-HRP or B3/25-gold. Incubating cells for 2 h in 1 mM dithiothreitol prevents newly synthesized chimeras from folding properly and becoming enzymatically active (Stinchcombe et al., 1995), allowing active chimeras to be chased from the biosynthetic pathway so that only chimeras recycling through the endosome are seen. Thus, the TR-HRP signal is very much stronger than that obtainable with Tf-HRP, and in thick (1.0-μm) sections, the asymmetric distribution of wild-type TR-HRP chimeras on the basolateral surface (Fig. 10 *e*) as well as the intracellular TR-containing elements were clearly displayed. In particular, it was evident that the 60-nm-diam tubules often formed branching networks (Fig. 10 *b*) in the immediate vicinity of the more irregularly shaped vacuole elements. There were sometimes extensions of the perimeter membrane which suggested that both the 60-nm and the 250-nm-diam tubules may be in continuity with the vacuole (Fig. 10 *c*). At the basolateral surface (Fig. 10, *d* and *e*), the plasma membrane was frequently invaginated to form strongly labeled coated pits and 60-nm-diam exocytotic profiles. In cells labeled from the apical surface, the lumina of these 60 nm diameter exocytic invaginations sometimes contained tracer but, in keeping with the view that these are exocytic rather than endocytic invaginations, there was no indication of a cytoplasmic coat (see Fig. 7 *c*). It should be added that while caveolae are frequently seen on the basolateral surface, they are readily distinguished from exocytotic profiles because they have a characteristic narrow neck and are unlabeled.

Discussion

All transcytotic pathways are thought to begin with internalization and delivery to an endosome compartment from which trafficking proteins either transfer across the cell or recycle back to the surface from which they were in-
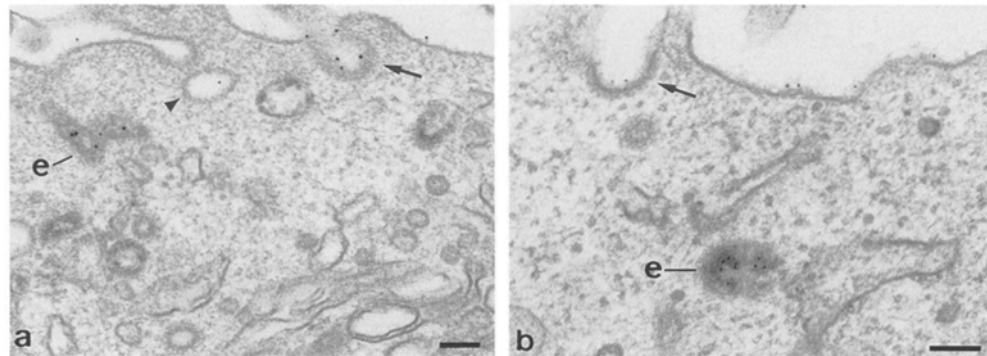
Figure 9. TRs enter the common endosome directly from the apical surface. Monolayers were loaded basolaterally with Tf-HRP at 37°C for 60 min. B3/25-gold was then bound apically at 5°C for 60 min. Monolayers were then rinsed free of unbound tracer and incubated at 37°C for 5 min. During the 5-min warm up, the B3/25-gold begins to internalize and is seen in coated pits (*arrows*), small vesicles without Tf-HRP (which are probably uncoated vesicles derived from clathrin-coated pits) (*arrowhead*) and Tf-containing endosomal elements (*e*). Note that the apical surface is free of Tf-HRP. Endosomal elements containing gold but lacking Tf-HRP are not observed. Bar, 0.2 μm.
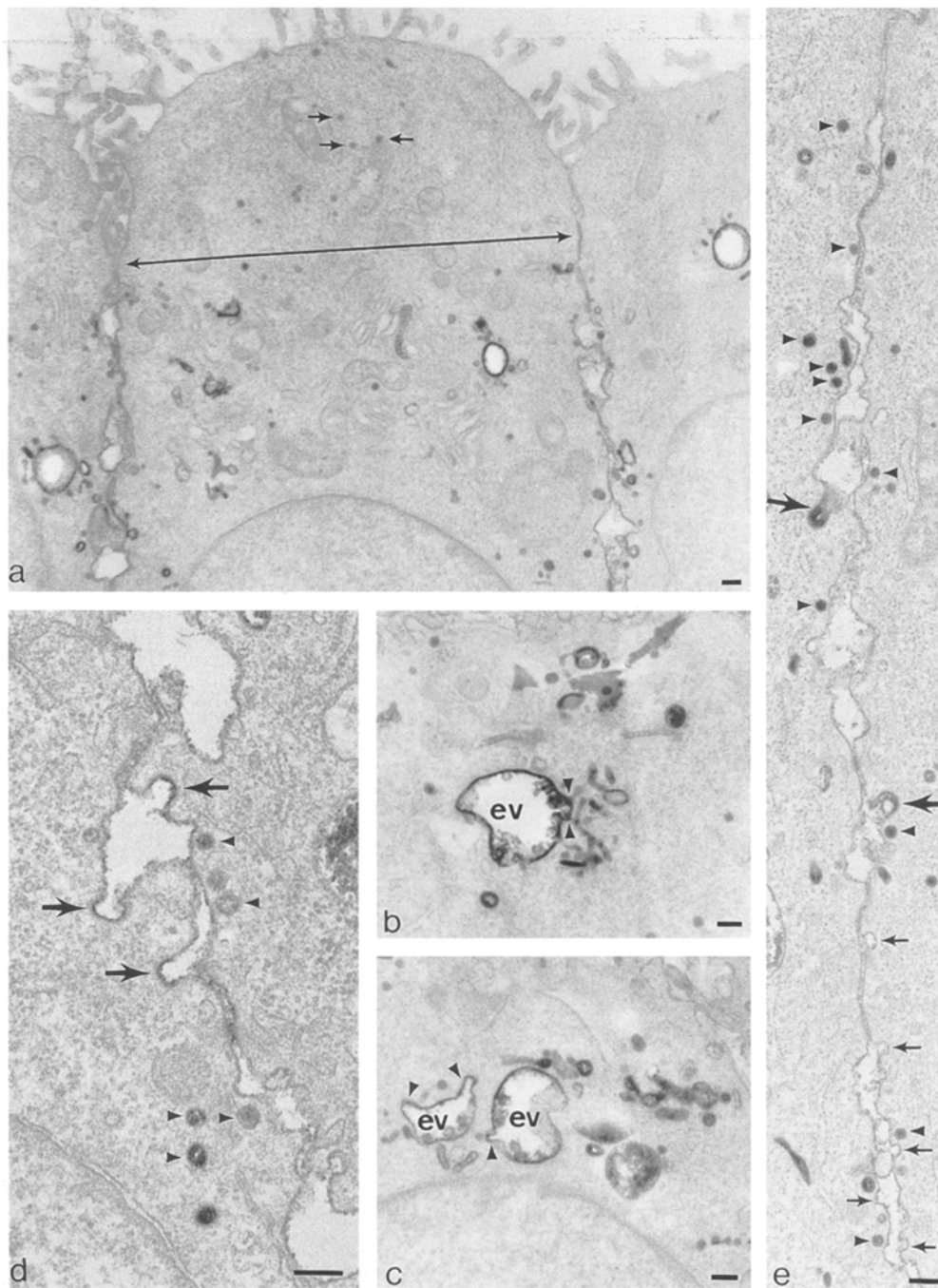
Figure 10. Thick sections of MDCK cells expressing wild-type TR-HRP chimeras show the distribution of endosomal elements and free 60-nm-diam vesicles. (*a–c*) Unstained, thick (1.0-μm) sections of monolayers expressing wild-type TR-HRP chimeras show the distribution of peroxidase reaction product. (*a*) Low power view; a line drawn at the level of the junction complexes is an example of the demarcation of apical and basolateral cytoplasm used for quantitation. (*b*) Endosomal vacuole (*ev*) and associated 250-nm-diam tubulo vesicles, indicating sites (*arrowheads*) at which tubulo vesicles may be connected to vacuole. (*c*) Endosomal vacuoles (*ev*) and branching 60-nm-diam tubules; arrowhead indicates continuity. (*d* and *e*) Thin sections showing expression of TR-HRP chimeras along the full-length of the basolateral border. Large arrows indicate coated pits, arrowheads indicate 60-nm-diam transcytotic vesicles, and small arrows indicate 60-nm-diam invaginations indicative of exocytosis. Bar, 0.2 μm.

ternalized (Schaerer et al., 1990; Sztul et al., 1991; Rodriguez-Boulan and Powell, 1992). Most current models have, therefore, proposed that the endocytic compartments of polarized cells contain polarized sorting mechanisms (Matter and Mellman, 1994). However, it is also generally believed that polarized cells, and in particular MDCK cells (Bomsel et al., 1989; Parton et al., 1989), contain separate apical and basolateral endosome compartments with independent transcytotic pathways to the opposite surface (Fig. 11 *A*). To maintain the polarized phenotype of membrane proteins such as TR which continually traffic between the basolateral and apical surfaces would require that the separate apical and basolateral en-

dosomes envisaged in this model each contain polarized sorting machinery. Coordinate regulation of both polarized sorting mechanisms would also be required. Our data suggest an alternative arrangement in which TRs internalized from either surface become rapidly and extensively codistributed within an interconnected endosomal system and that the preferential basolateral delivery of internalized TRs depends upon a polarized sorting mechanism which directs their transfer from this system to the basolateral surface (Fig. 11 *B*). This model has the important conceptual advantage in that the asymmetric surface distribution of TRs can be generated with reference to a single intracellular receptor pool.

A

B
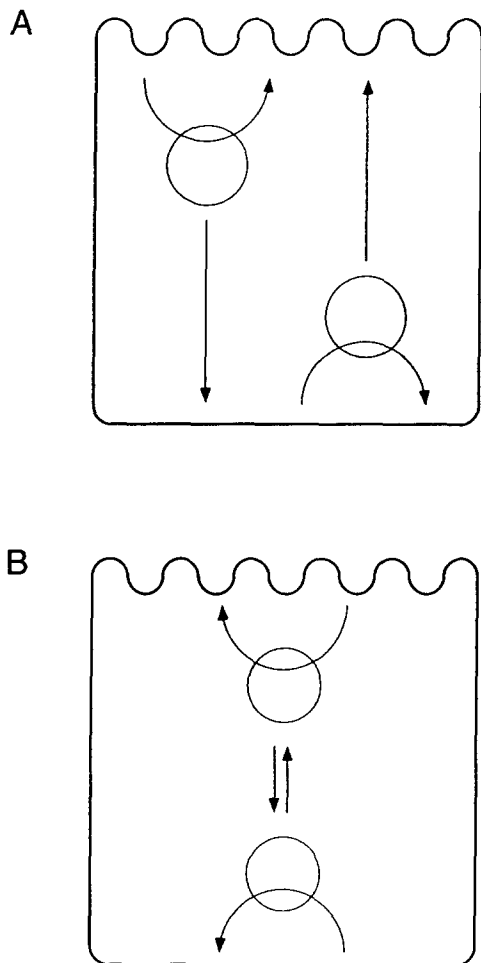
Figure 11. Models for recycling and transcytosis in MDCK cells. In *A*, transport between the apical and basolateral surfaces of MDCK cells is mediated by separate apical and basolateral endosomes. If these separate endosomes contain separate polarized sorting mechanisms they will need to operate in concert if they are to regulate a common pool of TRs. A simpler system is shown in *B*, in which apical and basolateral endosomes are interconnected and contain a single basolateral sorting mechanism. Our biochemical and morphological studies suggest that this polarized sorting machinery is associated with the more basolateral elements of this interconnected endosome system.

Two factors contributed to our ability to demonstrate that the basolateral and apical endocomes of MDCK cells are interconnected. First, we were able to express human TRs at levels that allowed us to load with tracers from the apical surface while maintaining a well-polarized phenotype. Second, because Tf dissociates rapidly from internalized TRs that return to the cell surface, the transcellular pathway can be filled to equilibrium with Tf-HRP directly loaded from the basolateral surface without a significant contribution from Tf-HRP bound to receptors that have been transcytosed and have re-entered the endocytic pathway from the apical surface. The ability of apically applied B3/25-HRP to cross-link ∼80% of the ^{125}I-labeled Tf loaded from the basolateral surface provides confirmatory biochemical evidence that most of the TRs internalized from the apical and basolateral surfaces gain access to the same

endosomal elements. Our finding that within 2 h, as steady-state conditions are approached, the monolayer can be loaded to similar levels with ^{125}I-labeled Tf from either surface further supports this view.

Recent studies have suggested that a separate apical endosomal compartment exists in MDCK cells which contains apically directed ligand-receptor complexes such as those for polymeric IgA en route to the apical surface, although the relationship between this compartment and endosomal elements accessible to TRs internalized from the basolateral border is unclear (Barroso and Sztul, 1994; Apodaca et al., 1994). Our experiments showing that B3/25-gold applied apically as a pulse rapidly enters elements containing basolaterally applied Tf give no indication of an intermediate compartment on the inward route from the apical surface to these elements. However, the rapid recycling of ^{125}I-labeled Tf applied apically as a 5-min pulse back to the apical surface implies that the basolateral sorting machinery is not symmetrically distributed throughout the endosomal system.

Biosynthetic routes to the surfaces of polarized cells have yet to be delineated morphologically, but studies of a range of secretory proteins which can be expected to be transported to the MDCK cell surface in a signal-independent manner clearly suggest that the volumes of vesicular traffic to the separate apical and basolateral surfaces in these cells are approximately equal (Kondor-Koch et al., 1985; Gottlieb et al., 1986b). The simplest explanation of the steady-state cell surface distributions, recycling, and biosynthetic cell surface delivery of wild-type and tailless TRs in MDCK cells is that the TR cytoplasmic tail contains a basolateral targeting signal and that when it is removed, receptors are transported randomly to both surfaces in a signal-independent fashion. The interpretation that signal-independent transport in MDCK cells is random is strengthened by the observation that the surface distributions of wild-type and tailless TR-HRP chimeras are indistinguishable from those of the wild-type and tailless TRs. A number of studies have shown that removal of the cytoplasmic domain (or ablation of the basolateral targeting signal) results in the asymmetric apical expression of other basolateral proteins. Although generally interpreted to mean that proteins lacking polarity signals move apically by default, our results support the alternative suggestion (Matter and Mellman, 1994; Fiedler and Simons, 1995) that these proteins contain residual apical targeting information.

Mutation of basolateral targeting signals has also been shown to alter the proportion of endocytosed proteins being transcytosed (Matter et al., 1993; Aroeti and Mostov, 1994). However, in these previous studies, it was not possible to load MDCK endosome compartments to a level approaching steady state, so the relative kinetics of traffic to the different surfaces could not be compared.

As with their biosynthetic delivery, the recycling of internalized tailless TRs in the endocytic system approximates that of a freely mobile protein being randomly routed along both basolateral and apical pathways. Fluid-phase HRP, for example, when internalized from the apical surface of MDCK cells, like the tailless TR, reaches the apical and basolateral surfaces in equal amounts (Bomsel et al., 1989). When set against this unpolarized background,

the delivery of 70–90% of internalized wild-type TRs to the basolateral border (depending upon which side tracer is loaded) is clearly strongly polarized and is probably sufficient to generate and maintain the asymmetric expression of the receptor seen on the separate cell surfaces at steady state.

Evidence for a signal-independent recycling pathway in MDCK cells, analogous to the signal-independent recycling pathways described in nonpolarized cells (Jing et al., 1990; Mayor et al., 1993; Hopkins et al., 1994), is provided by our data on the short-term kinetics of recycling of ^{125}I-labeled Tf at the apical surface. A similar signal-independent recycling pathway presumably operates at the basolateral border in addition to the signal-dependent machinery that mediates polarized sorting. Studies of the signal-independent and -dependent trafficking of TRs in nonpolarized cells showed that both tailless and wild-type TRs enter the same clathrin-coated pit, but without an internalization signal, the efficiency of recruitment of tailless TRs is reduced to 10–15% of wild-type (Jing et al 1990; Miller et al., 1991). It is not necessary, therefore, to propose that the different pathways use separate populations of vesicles that transfer them to the cell surface; tailless TRs could be incorporated into the same 60-nm-diam vesicles as wild-type TRs provided that a sorting mechanism such as a clathrin-coated domain was operating and could increase the efficiency of recruitment of the wild-type receptor.

Studies on living nonpolarized cells suggest that the movement of receptors within endosome compartments is iterative rather than vectorial (Dunn et al., 1989), so that receptors destined for the lysosome gradually accumulate within sorting endosome vacuoles like MVB, while receptors like TR, which are destined to recycle back to the cell surface, are transferred to 60-nm-diam tubules (Hopkins et al., 1990, 1994; Futter et al., 1996). The distributions of internalized tracers we have observed in MDCK cells are presumably generated by similar mechanisms so that while they rapidly distribute throughout the vacuoles and tubules of the entire endosome, they concentrate within the 60-nm-diam tubules in preparation for delivery to the surface. Recently, Stoorvogel et al. (1996) have shown that branching endosomal tubules containing TRs, which are morphologically similar to those we have identified in MDCK cells, bear clathrin-coated buds having diameters of ~50 nm. These domains, however, could not be shown to concentrate TRs (Stoorvogel et al., 1996), but in polarized MDCK cells, it is possible that similar buds have the ability to bind TRs. Selective entrapment of TRs within coated buds of the endosome could thus be responsible for concentrating and packaging these receptors into the 60-nm-diam vesicles we have observed carrying recycling and transcytosing receptors to the basolateral border.

From the kinetics of recycling and transcytosis of ^{125}I-labeled Tf to the apical and basolateral surfaces of MDCK cells, we propose a model for processing of TRs within the interconnected endosome compartments of polarized cells which has the essential features of TR processing seen in nonpolarized cells. As shown in Fig. 11 B, TRs internalized from both the apical and basolateral surfaces enter an endosome compartment from which they can rapidly recycle in a signal-independent manner. With continuous loading from the apical surface, Tf which is

bound to TRs displaying a basolateral targeting signal will be selectively captured by the polarized sorting mechanism which ensures that they enter the pathway to the basolateral border. Similar short and long circuits for TR trafficking within the endosome compartment of nonpolarized cells have been demonstrated (Hopkins et al., 1990), but there is, as yet, no indication that a signal-dependent transfer occurs at an intracellular location in these cells.

In summary, we have presented evidence supporting a simplified model for polarized sorting in MDCK cells (Fig. 11 B). This model postulates that a signal-dependent polarized sorting mechanism located within an endosome system accessible to both apical and basolateral surfaces is both necessary and sufficient to maintain the polarized phenotype.

References

Apodaca, G., L.A. Katz, and K.E. Mostov. 1994. Receptor-mediated transcytosis of IgA in MDCK cells is via apical recycling endosomes. *J. Cell Biol.* 125: 67–86.

Aroeti, B., and K.E. Mostov. 1994. Polarized sorting of the polymeric immunoglobulin receptor in the exocytotic and endocytotic pathways is controlled by the same amino acids. *EMBO (Eur. Mol. Biol. Organ.) J.* 13:2297–2304.

Aroeti, B., P.A. Kosen, I.D. Kuntz, F.E. Cohen, and K.E. Mostov. 1993. Mutational and secondary structural analysis of the basolateral sorting signal of the polymeric immunoglobulin receptor. *J. Cell Biol.* 123:1149–1160.

Barroso, M., and E.S. Sztul. 1994. Basolateral to apical transcytosis in polarized cells is indirect and involves BFA and trimeric G protein sensitive passage through the apical endosome. *J. Cell Biol.* 124:83–100.

Bates, P., J.A.T. Young, and H.E. Varmus. 1993. A receptor for subgroup A Rous sarcoma virus is related to the low density lipoprotein receptor. *Cell.* 74:1043–1051.

Bomsel, M., K. Prydz, R.G. Parton, J. Gruenberg, and K. Simons. 1989. Endocytosis in filter-grown Madin–Darby canine kidney cells. *J. Cell Biol.* 109: 3243–3258.

Dunn, K.W., T.E. McGraw, and F.R. Maxfield. 1989. Iterative fractionation of recycling receptors from lysosomally destined ligands in an early sorting endosome. *J. Cell Biol.* 109:3303–3314.

Fiedler, K., and K. Simons. 1995. The role of N-glycans in the secretory pathway. *Cell.* 81:309–311.

Futter, C.E., C.N. Connolly, D.F. Cutler, and C.R. Hopkins. 1995. Newly synthesised transferrin receptors can be detected in the endosome before they appear on the cell surface. *J. Biol. Chem.* 270:10999–11003.

Futter, C.E., A. Pearse, L.J. Hewlett, and C.R. Hopkins. 1996. Multivesicular endosomes containing internalized EGF–EGF receptor complexes mature and then fuse directly with lysosomes. *J. Cell Biol.* 132:1011–1023.

Gottlieb, T.A., A. Gonzalez, L. Rizzolo, M.J. Rindler, M. Adesnik, and D.D. Sabatini. 1986a. Sorting and endocytosis of viral glycoproteins in transfected polarized epithelial cells. *J. Cell Biol.* 102:1242–1255.

Gottlieb, T.A., G. Beaudry, L. Rizzolo, A. Colman, M. Rindler, M. Adesnik, and D.D. Sabatini. 1986b. Secretion of endogenous and exogenous proteins from polarized MDCK cell monolayers. *Proc. Natl. Acad. Sci. USA.* 83: 2100–2104.

Hopkins, C.R. 1985. The appearance and internalization of transferrin receptors at the margins of speading human tumor cells. *Cell.* 40:199–208.

Hopkins, C.R., and I.S. Trowbridge. 1983. Internalization and processing of transferrin and the transferrin receptor in epidermoid carcinoma cells. *J. Cell Biol.* 97:508–521.

Hopkins, C.R., A Gibson, M. Shipman, and K. Miller. 1990. Movement of internalized ligand-receptor complexes along a continuous endosomal reticulum. *Nature (Lond.).* 346:335–339.

Hopkins, C.R., A. Gibson, M. Shipman, D.K. Strickland, and I.S. Trowbridge. 1994. In migrating fibroblasts, recycling receptors are concentrated in narrow tubules in the pericentriolar area, and then routed to the plasma membrane of the leading lamella. *J. Cell Biol.* 125:1265–1274.

Hughson, E.J., and C.R. Hopkins. 1990. Endocytic pathways in polarized caco-2 cells: identification of an endosomal compartment accessible from both apical and basolateral surfaces. *J. Cell Biol.* 110:337–348.

Ikonen, E., M. Tagaya, O. Ullrich, C. Montecucco, and K. Simons. 1995. Different requirements for NSF, SNAP, and rab proteins in apical and basolateral transport in MDCK cells. *Cell.* 81:571–580.

Jing, S., T. Spencer, K. Miller, C. Hopkins, and I.S. Trowbridge. 1990. Role of the human transferrin receptor cytoplasmic domain in endocytosis: localization of a specific signal sequence for internalization. *J. Cell Biol.* 110:283–294.

Karnovsky, M.J. 1965. A formaldehyde–glutaraldehyde fixative of high osmolarity for use in electron microscopy. *J. Cell Biol.* 27:137.

Knight, A., E. Hughson, C.R. Hopkins, and D.F. Cutler. 1995. Membrane protein trafficking through the common apical endosome in Caco-2 cells. *Mol. Biol. Cell.* 6:597–610.

Kondor-Koch, C., R. Bravo, S.D. Fuller, D. Cutler, and H. Garoff. 1985. Exocytotic pathways exist to both the apical and the basolateral cell surface of the polarized epithelial cell MDCK. *Cell.* 43:297–306.

Kornfeld, S., and I. Mellman. 1989. The biogenesis of lysosomes. *Annu. Rev. Cell Biol.* 5:483–525.

Leitinger, B., A. Hille-Rehfeld, and M. Spiess. 1995. Biosynthetic transport of the asialoglycoprotein receptor H1 to the cell surface occurs via endosomes. *Proc. Natl. Acad. Sci. USA.* 92:10109–10113.

Matter, K., and I. Mellman. 1994. Mechanisms of cell polarity: sorting and transport in epithelial cells. *Curr. Opin. Cell Biol.* 6:545–554.

Matter, K., J.A. Whitney, E.M. Yamamoto, and I. Mellman. 1993. Common signals control low density lipoprotein receptor sorting in endosomes and the Golgi complex of MDCK cells. *Cell.* 74:1053–1064.

Mayor, S., J.F. Presley, and F.R. Maxfield 1993. Sorting of membrane components from endosomes and subsequent recycling to the cell surface occurs by a bulk flow process. *J. Cell Biol.* 121:1257–1269.

McClelland, A., L. Kuhn, and F.H. Ruddle. 1984. The human transferrin receptor gene: genomic organization, and the complete primary structure of the receptor deduced from a cDNA sequence. *Cell.* 39:267–274.

Miller, K., M. Shipman, I.S. Trowbridge, and C.R. Hopkins. 1991. Transferrin receptors promote the formation of clathrin lattices. *Cell.* 65:621–632.

Mostov, K., G. Apodaca, B. Aroeti, and C. Okamoto. 1992. Plasma membrane protein sorting in polarized epithelial cells. *J. Cell Biol.* 116:577–583.

Naim, H.Y., D.T. Dodds, C.B. Brewer, and M.G. Roth. 1995. Apical- and basolateral-coated pits of MDCK cells differ in their rates of maturation into coated vesicles, but not in the ability to distinguish between mutant hemagglutinin proteins with different internalization signals. *J. Cell Biol.* 129:1241–1250.

Odorizzi, G., and I.S. Trowbridge. 1994. Recombinant Rous sarcoma virus vectors for avian cells. *Methods Cell Biol.* 43:79–97.

Odorizzi, C.G., I.S. Trowbridge, L. Xue, C.R. Hopkins, C. Davis, and J.F. Collawn. 1994. Sorting signals in the MHC class II invariant chain cytoplasmic tail and transmembrane region determine trafficking to an endocytic processing compartment. *J. Cell Biol.* 126:317–330.

Parton, R.G., K. Prydz, M. Bomsel, K. Simons, and G. Griffiths. 1989. Meeting of the apical and basolateral endocytic pathways of the Madin–Darby canine kidney cell in late endosomes. *J. Cell Biol.* 109:3259–3272.

Rodriguez-Boulan, E., and S.K. Powell. 1992. Polarity of epithelial and neuronal cells. *Annu. Rev. Cell Biol.* 8:395–427.

Schaerer, E., M.R. Neutra, and J.P. Kraehenbuhl. 1991. Molecular and cellular mechanisms involved in transepithelial transport. *J. Memb. Biol.* 123:93–103.

Simons, K., and A. Wandinger-Ness. 1990. Polarized sorting in epithelia. *Cell.* 62:207–210.

Slot, J.W., and H.J. Geuze. 1985. A new method for preparing gold probes for multiple labeling cytochemistry. *Eur. J. Cell Biol.* 38:87–93.

Stinchcombe, J., D. Cutler, and C.R. Hopkins. 1995. Anterograde and retrograde traffic between the rough endoplasmic reticulum and the Golgi complex. *J. Cell Biol.* 131:1387–1401.

Stoorvogel, W., V. Oorschot, and H.J. Geuze. 1996. A novel class of clathrin-coated vesicles budding from endosomes. *J. Cell Biol.* 132:21–33.

Sztul, E., A. Kaplin, L. Saucan, and G. Palade. 1991. Protein traffic between distinct plasma membrane domains: isolation and characterization of vesicular carriers involved in transcytosis. *Cell.* 64:81–89.

Urban, J., K. Parczyk, A. Leutz, M. Kayne, and C. Kondor-Koch. 1987. Constitutive apical secretion of an 80-kD sulfated glycoprotein complex in the polarized epithelial Madin–Darby canine kidney cell line. *J. Cell Biol.* 105:2735–2743.

Weibel, E.R. 1979. Stereological Methods, Practical Methods for Biological Morphometry. Academic Press, Inc., New York.

White, S., K. Miller, C. Hopkins, and I.S. Trowbridge. 1992. Monoclonal antibodies against defined epitopes of the human transferrin receptor cytoplasmic tail. *Biochem. Biophys. Acta.* 1136:28–34.